INTERACTION OF DIFFERENT WAVELENGTHS IN A TURBULENT FLOW WITHIN A RANDOM ARRAY OF RIGID AND EMERGENT STEMS

Ana M. Ricardo[1], M. Franca[2], A. Schleiss[3] and R. Ferreira[4]

[1]CEHIDRO - IST - TULisbon, Portugal & LCH - EPFLausanne, Switzerland
E-mail : ana.ricardo@ist.utl.pt
[2] Faculty of Sciences and Technology & IMAR- CMA, New University of Lisbon, Caparica, Portugal
[3]LCH - Ecole Polytechnique Fédérale de Lausanne, Switzerland
[4]CEHIDRO - Instituto Superior Técnico - Techical University of Lisbon, Portugal

Abstract

Emergent vegetation covering floodplains and wetlands has an important role in fluvial ecosystems. Since natural systems are not homogeneous, the flow within the stem array is influenced by several space scales, determined by the number-density of stems and its spatial modulation. The aim of this study is to characterize experimentally the spatial variation of the flow at the smallest spatial scales over a wavelength of the largest scale. To meet the proposed objectives, an experimental test was carried out where two stem's densities were alternated with a fixed period, allowing the interaction of three different wavelengths: two different inter-stem spaces and the characteristic length between the two densities. The measurements of velocity fields were made using Particle Image Velocimetry (PIV). The data treatment was done with the Double Averaged methodology (DAM) to account for the great spatial variability of the flow.

Keywords: Emergent vegetation, rigid stems, spatial heterogeneity, double-averaging, PIV

Introduction

River engineering works procure, in a sustainable society, not only flood protection but also the promotion of high standards of water quality and habitat diversity, within good landscape design practices. Emergent vegetation covering wetlands has an important role in fluvial ecosystems being able to control the fluxes of sediment, nutrients and contaminants (Tanino and Nepf 2008). The characteristics of the flow, namely velocities, stresses and fluxes, are strongly dependent on the density and type of vegetation. The plants exhibit a wide morphological range, from naked stems (i.e. jonquil or young willow) to dense foliages (adult willow), and dynamic behavior (rigid or flexible stems). In addition, vegetation characteristics change diachronically, expressing growth stage and seasonality. Such morphological diversity justifies the smaller body of knowledge about these flows compared to boundary layer flows. Progresses have been made in the characterization of 3D flows over irregular boundaries and canopies, mainly due to the application of double-averaging methods (DAM), which are a particular form of upscaling in the spatial and temporal sense (Gimenez-Curto and Corniero Lera 1996, Finnigan 2000 and Nikora et al. 2001, 2007). Such methods are especially pertinent for the characterization of the flow within and in the near vicinity of plant canopies.

Since the spatial distribution of plant stems is, in general, not uniform, the flow within the stem array is influenced by several space scales, determined by the number-density of stems and its spatial modulation. The aim of this study is to characterize experimentally the spatial variation of the flow at the smallest spatial scales over a wavelength of the largest scale. To meet the proposed objectives, an experimental test was carried out where two stem densities were alternated with a fixed wavelength, allowing the interaction of three different wavelengths: two different inter-stem spaces and the characteristic length between the two densities. The measurements of velocity fields were made using Particle Image Velocimetry (PIV). The data treatment was done with the Double Averaging methodology to account for the great spatial variability of the flow. The conservation equations of turbulent flows are expressed for time-averaged quantities which, in case of unsteady flow, are defined in a time-window smaller than the fundamental unsteady flow time-scale, and for space

averaged quantities, defined in space windows larger than the characteristic wavelength of the boundary irregularities.

The data treatment was performed in order to allow the computation of the terms of the momentum conservation equation, namely, convective acceleration, Reynolds and form induced stresses.

Laboratory Facilities

The data presented in this text resulted from an experimental test carried out in a 12.5 m long and 0.408 m wide tilting recirculation flume of the Laboratory of Hydraulics of IST. The flume has glass side walls, enabling flow visualization and laser measurements (Figure 1). The flume bottom was covered with a thin horizontal layer of gravel and sand and arrays of rigid, vertical and cylindrical stems were randomly placed along of a 3.5 m long reach simulating emergent vegetation conditions. The stems were placed in order to create patches with a higher density (≈1600 stems/m^2) alternated with patches of lower density (≈400 stems/m^2).

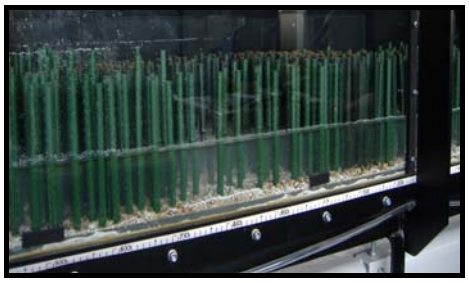

Figure 1 – Flume view during experiments.

Both of these reaches have the flume width and a length of 15 cm and they are separated by a 10 cm long transition reach where the stem density is 1200 stems/m^2 along half of the reach and it is 800 stems/m^2 on the another half. Figure 2 is a plan view of the downstream part of the vegetation-covered reach, which included the 8 longitudinal positions where vertical and horizontal instantaneous maps of velocity were measured. Downstream the vegetation covered reach a coarse gravel weir controlled the flow.

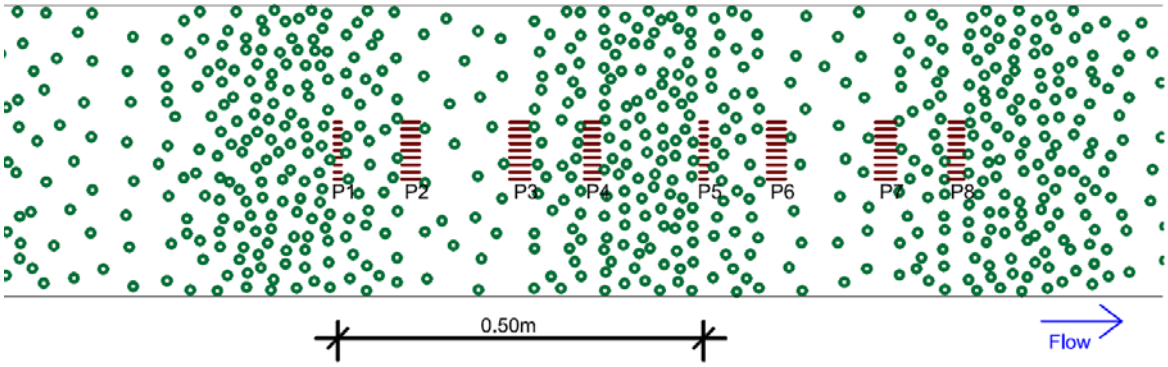

Figure 2 - Plan view of part of the vegetation covered reach. The horizontal brown lines represent the positions where the vertical measurements were made on.

Instantaneous velocity maps were obtained with a 532 nm, 30 mJ 2D Particle Image Velocimetry (PIV) system. The PIV is an optical technology that allows the obtaining of the fluid velocity by measuring seeding particle velocity. The system is composed of laser head, power supply, CCD camera and acquisition system and control and it is based on a double-cavity laser which allows the user to set the delay between two laser pulses. During these experimental tests the PIV was operated at a sampling rate of 15 Hz and with a time between pulses of 1500 μs. Polyurethane seeding particles were employed for flow visualization and measuring. Its specific gravity is 1.31 and the diameters range is from 50 to 70 μm, with 60 μm of mean. Using this seeding, the cut-off frequency of the turbulent signal, calculated with the theory of Hjemfelt and Mockros (1996), is about 40 Hz. Given that the Nyquist frequency of the time series obtained with the PIV is 7.5 Hz, it is concluded that the seeding particles are adequate for the performed laboratory work.

For each longitudinal position, represented in Figure 2 (P1-P8), measurements were made in one horizontal plane and in 9 vertical planes (identified by the brown horizontal lines on Figure 2). For each position 10x573 image couples were collected, representing a total acquisition time of 6′37″.

Qualitative description of the flow

This section presents a general description of the flow variables at each longitudinal position and a qualitative description of the flow behaviour within a dense array of stems based on the mean velocity

maps. The tests were performed with a discharge of 2.33 ls^{-1}. In Table 1, x stands for the distance between the flume inlet and each position (longitudinal spatial coordinate), h is the time-averaged flow depth, dh/dx is the longitudinal gradient of flow depth, U is the depth average of mean velocity for the depth where the flow is controlled by the stems, m represents the stem density and $Re_p=Ud/v$ is the stems Reynolds number, where d stands for stem diameter. A longitudinal profile of the bed topography and the free surface are presented in Figure 3, where each point is the cross section average value. The free surface and the bed levels were surveyed by means of a CCD laser displacement sensor.

Table 1 - Flow properties for each longitudinal position.

	x (cm)	h (m)	dh/dx (-)	U (m/s)	Re_p (-)	m (stems/m^2)
P1	6.680	0.066	-0.014	0.087	1145	1600
P2	6.780	0.063	-0.027	0.091	1201	800
P3	6.920	0.062	-0.010	0.093	1224	400
P4	7.030	0.061	-0.009	0.094	1237	1200
P5	7.180	0.056	-0.033	0.103	1355	1600
P6	7.290	0.054	-0.016	0.106	1395	800
P7	7.440	0.053	-0.008	0.108	1421	400
P8	7.530	0.052	-0.008	0.111	1460	1200

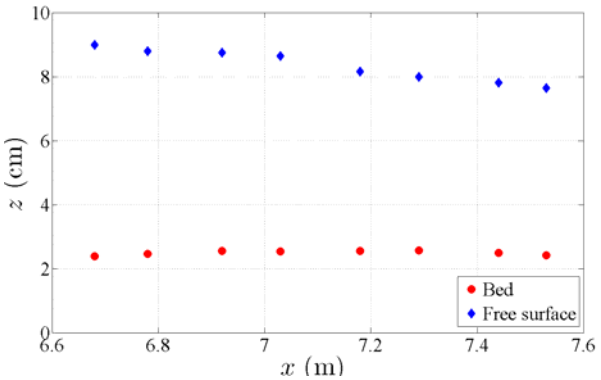

Figure 3 - Longitudinal profile of bed and free surface level.

Figure 3 shows that the flow is gradually varied, accelerating in the downstream direction as the flow depth decreases. Furthermore, one can observe a higher head loss from P4 to P5, which correspond to a reach with higher stem density where the flow resistance is higher.

Maps of 2D horizontal mean velocity (Figures 5 to 8 a) and maps of mean vorticity (Figures 5 to 8 b) were computed to characterize the flow in the inter-stem region for all the longitudinal positions. These maps show that the flow within vegetation covered areas is extremely heterogeneous, with lower velocity in the wake of the stems and higher velocity in regions between two stems.

In the vorticity maps, one can observe a repeating pattern of paired vortexes caused by the unsteady separation of the flow provoked by the stems. These quasi-symmetric high vorticity patterns behind the stems identify Von Kármán vortex streets. Comparing vorticity maps for the different longitudinal positions, which correspond for different mean inter-stem spaces, one can conclude that stems induce quite regular structure of vortex patterns independently of the stem density. The main difference is that the space necessary to fully develop the vortex pattern is strongly reduced in the higher density. At higher stem densities, the vortex pattern is forced to compress due to the proximity of the next stem, while at positions with larger mean inter-stems scale (lower stem density) the vortex pattern has space to develop a vortex street once the next stem is far enough.

The color graphs presented in Figure 8 are two examples of mean vertical velocity fields computed for 9 lateral sections (y = 16.4; 17.4; 18.4; 19.4; 20.4; 21.4; 22.4; 23.4 and 24.4 cm) in each longitudinal position. With these maps, the double averaged methodology was applied to compute the time and spatial average flow variables, which are presented in the next section.

Results

After the double average analysis for each longitudinal position, a phase average was computed for the position with the same stem density. Hereinafter the acronyms PA1, PA2, PA3 and PA4 are used to indicate the average in P1 and P5, P2 and P6, P3 and P7, P4 and P8, respectively. The background of the next figures represents the variation of the stem density in order to render clearer the effect of the density of stems on the flow variables. To produce dimensionless graphs, it was used H, the depth of the flow controlled by the vertical elements, as characteristic length, and U, the average of the longitudinal velocity within the depth H as kinematic scale.

Figure 9 shows the longitudinal, $\langle \overline{u} \rangle$ (up) and the vertical, $\langle \overline{w} \rangle$ (down) double average velocities for the different inter-stem spaces.

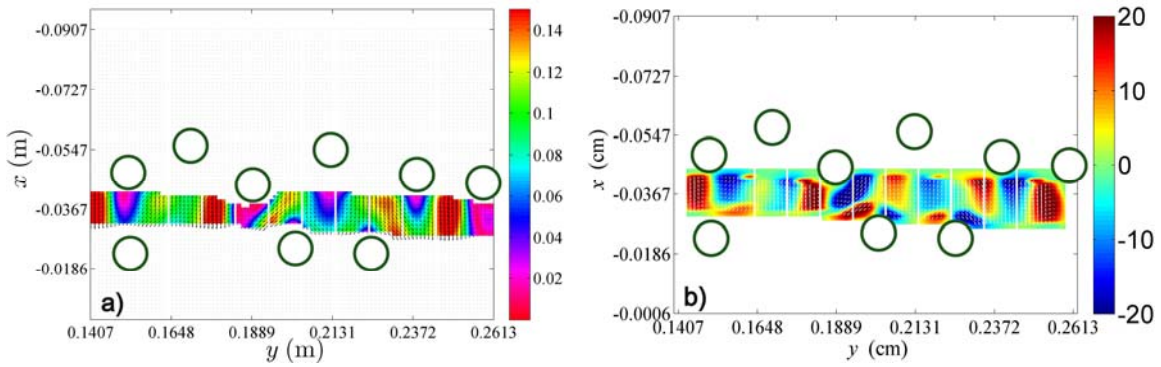

Figure 4 – a) Horizontal mean velocity map (m/s) at P1; b) vorticity map (s^{-1}) based on mean flow field at P1. Circles represent the nearest stems and the vertical white lines indicate the lateral positions where the vertical measurements were acquired. In these graphs, *x* represents a local reference for the flow direction and *y* stands for the transversal coordinate indicating the distance to the right side wall of the flume. The longitudinal position P5 presents a similar result.

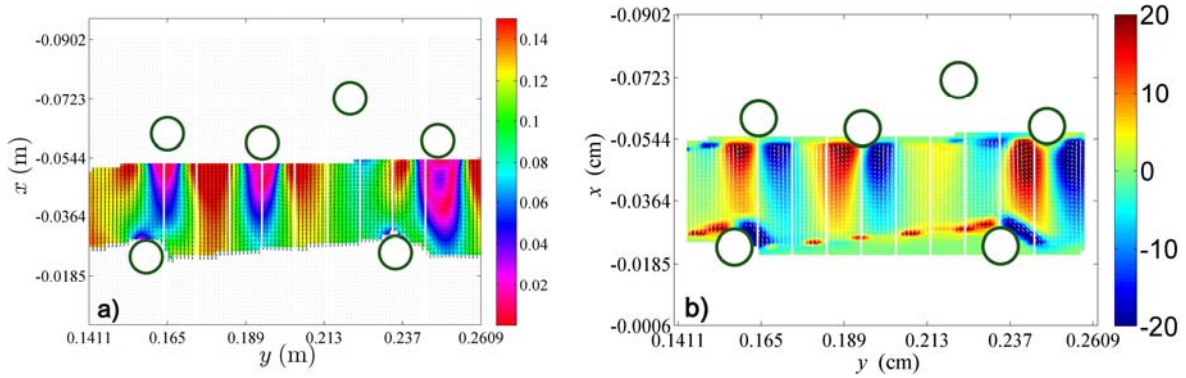

Figure 5 – Horizontal mean velocity (a)) and vorticity (b)) at position P2.

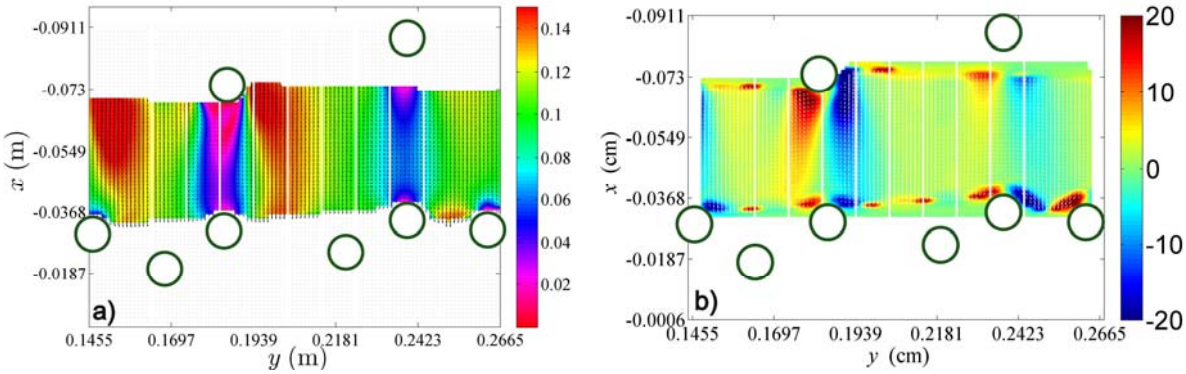

Figure 6 - Horizontal mean velocity (a)) and vorticity (b)) at position P3.

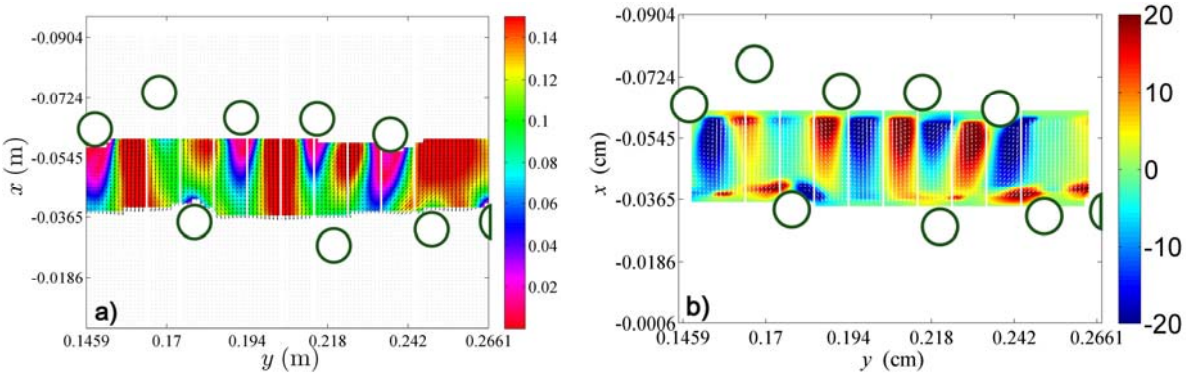

Figure 7 - Horizontal mean velocity (a)) and vorticity (b)) at position P4.

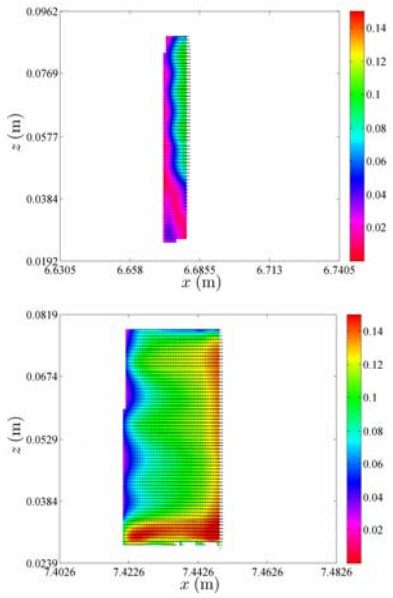

Figure 8 - Examples of vertical velocity fields. Left: P1 at y=19.4 cm; right: P7 at y=21.4 cm (cf. Fig.2 for the location of profiles).

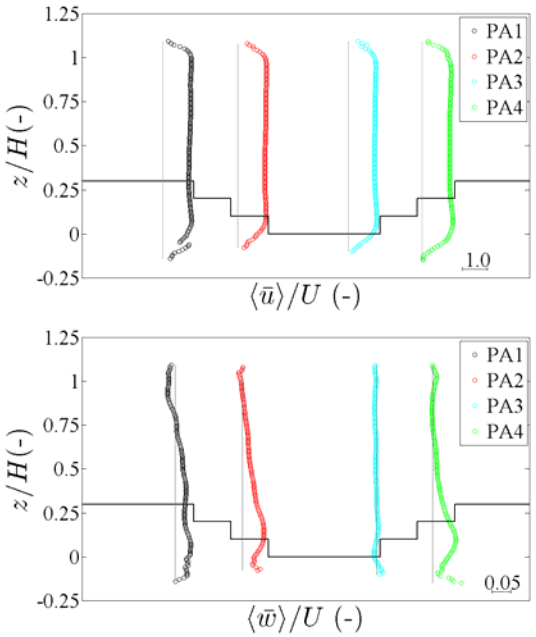

Figure 9 - Up: double average (DA) longitudinal velocity profiles; Down: DA vertical velocity profiles. Black line stands for relative stem density

One observes that the profiles of longitudinal velocity remain similar, with constant values in the reach where the flow is controlled by the vegetation elements. Furthermore, the graph shows that longitudinal velocity is almost constant for all the tested stem densities. Concerning vertical velocity, the profiles show that it is very close to zero values, as it was expected. The higher values appear due to effect of the bottom.

The profiles of the Reynolds shear stress, $\langle \overline{u'w'} \rangle$ and form-induced shear stress, $\langle \tilde{u}\tilde{w} \rangle$ are presented in Figure 10. Both stresses have the same order of magnitude with the maximum values near the bottom and becoming almost zero at levels close to the free surface, but form induced stresses are, in general, larger than Reynolds stresses. One can also observe that those stresses increase with the stem density.

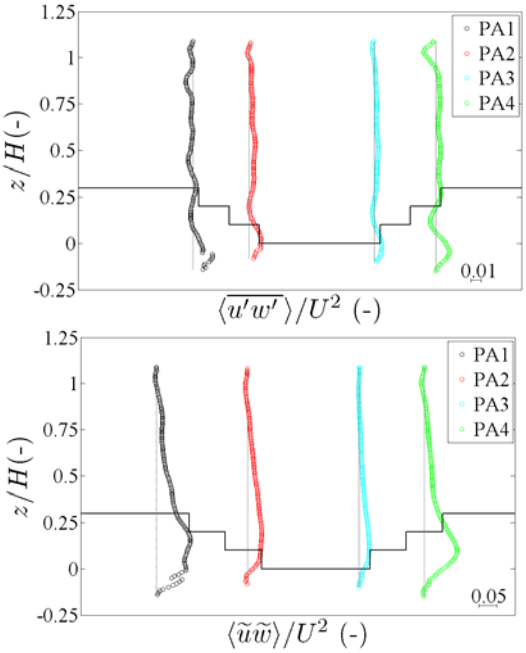

Figure 10 - DA shear stress profiles: up: Reynolds; down: form-induced.

Figure 11 presents the normal components of the form induced stress tensor.

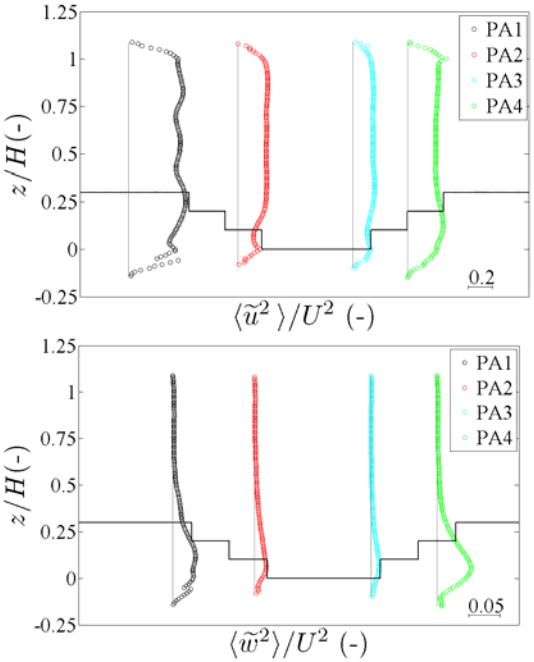

Figure 11 - DA form-induced normal profiles: up: longitudinal; down: vertical.

The longitudinal component, $\left\langle \tilde{u}^2 \right\rangle$ which represents the correlation of the spatial fluctuation of the longitudinal velocity with itself, is a good variable to translate the great heterogeneity of the flows within vegetation patches. The increase of this variable with increasing stem density is clear. The profiles of form-induced normal vertical stresses, $\left\langle \tilde{w}^2 \right\rangle$, show larger values near the bottom decreasing towards to free surface. This term signals the flow regions where the flow is 3D, with important vertical flow components. Its values peak in the overlapping region between the near-bed layer mostly influenced by bed roughness and the layer where the flow is determined by stem diameter and density. Furthermore, a correlation between the increasing of the form-induced normal vertical stresses with the stem density is also clear. The normal components of the turbulent stresses are presented in Figure 12.

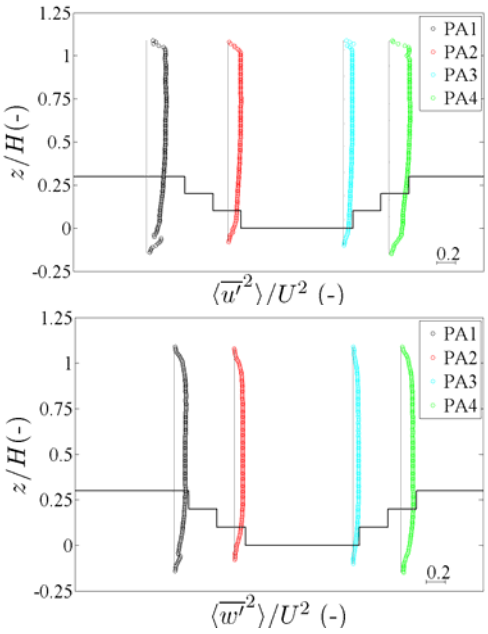

Figure 12 - DA Reynolds normal profiles: up: longitudinal; down: vertical.

It is observed that the longitudinal, $\left\langle \overline{u'}^2 \right\rangle$, and the vertical, $\left\langle \overline{w'}^2 \right\rangle$, components, have similar values, increasing with the stem density.

Conclusions

The characterization of the studied flow shows a great heterogeneity of flows within vegetation covered boundaries. One can conclude that the flow within a dense array of stems leads a quasi-symmetric high vorticity patterns around the stems independently of the stem density. However, stem density impacts the length of the vortex street: for lower densities the inter-stem space is larger allowing the development of the vortex street.

In what concerns the DA flow variables, the main conclusions are:

- There is a strong correlation between stem density and the magnitude of flow variables. Both turbulent and the form induced stresses increase with the density of the vertical elements.
- Form-induced stresses cannot be neglected compared with Reynolds stresses; they have the same order of magnitude.
- Normal longitudinal stresses are dominant; the form-induced component is larger than the Reynolds component.
- Normal longitudinal form-induced stresses are the main expression of flow heterogeneity and spatial anisotropy.
- Flow complexity increases towards the bed, expressed by the increase of form-induced shear and normal vertical stresses.

It should be noticed that the results and the conclusions presented in this work are the first steps in a work to understand the quite complex interaction of different wavelengths in flows over vegetation covered boundaries. Advances on spatial heterogeneity and more conclusions are expected soon.

Acknowledgements

The study was partly funded by the Portuguese Foundation for Science and Technology (FCT), project PTDC/ECM/099752/2008 and grant SFRH/BD/33668/2009

References

Finnigan, J. (2000). Turbulence in plant canopies. Annu. Rev. Fluid Mech. 32, 519–571.

Giménez-Curto, L. and M. Corniero Lera (1996). Oscillating turbulent flow over very rough surfaces. J. Geophys. Res. 101, 20745-20758.

Hjemfelt, A. T. and L. F. Mockros (1996). *Motion of discrete particles in a turbulent fluid*. Applied Science Research 16, 149-161.

Nikora, V., Goring, D., McEwan, I. and Griffiths, G. (2001). *Spatially averaged open-channel flow over rough bed*. Journal of Hydraulic Engineering 127(2), 123–133.

Nikora, V., McEwan, I., McLean, S., Coleman, S., Pokrajac, D. and Walters, R. (2007). *Double-averaging concepts for rough-bed open-channel and overland flows: Theoretical background*. Journal of Hydraulic Engineering 133(8), 873–883.

Tanino, Y. and H. M. Nepf (2008). *Lateral dispersion in a random cylinder array at high Reynolds number*, J. Fluid Mech., 600, 339-371.